

IMECE2006-14940

MODELING AND SIMULATION OF A SURFACE MICROMACHINED KNUDSEN PUMP

Naveen K. Gupta* and Yogesh B. Gianchandani**

*Department of Mechanical Engineering

**Department of Electrical Engineering and Computer Science
University of Michigan, Ann Arbor, MI-48109, USA

ABSTRACT

This paper presents a simulation model for a silicon micromachined Knudsen pump that combines analytical and numerical methods. It involves numerical modeling of the thermal response, followed by an analytical estimate of the pumping using Kennard's model. The loss of performance resulting from gas diffusion through walls of the pump is specifically addressed. The results are subsequently validated against the previously reported experimental measurements of a single-stage Knudsen pump. This device, which has a total footprint of less than $1500 \times 2000 \mu\text{m}^2$, has multiple narrow channels connecting two cavities, one of which is heated. This cavity is further connected through a wide channel to a third cavity, which remains at ambient. The simulation model for this device predicts a vacuum pressure of 0.47 atm. at an input power of 97.6 mW, which deviates less than 20% from the experimentally observed data. Finally, the paper extends the concept of single stage pumping to a multi-stage pump. While Kennard's model is used for modeling the first stage, the simulation for subsequent stages, which are characterized by a relatively high Knudsen number, uses an empirically corrected correlation by Knudsen.

I. INTRODUCTION

In 1879, Osborne Reynolds presented an explanation [1] for a phenomenon that was first observed (in 1873) by an eminent Victorian experimenter Sir William Crookes and coined the term 'thermal transpiration' for it. Reynolds' work was followed in the same year by a rigorous mathematical analysis by Maxwell [2]. The principle of thermal transpiration has its observable effects at submicron scales, i.e. when the hydraulic diameter of a channel much less than the mean free path of the gas flowing through it. Near atmospheric pressure,

these channels must have hydraulic diameter on the order of 100 nm or less. The flow through these channels is characterized by the transitional or free molecular flow regime [3], and continuum physics is inadequate. It was not until Knudsen's work in 1910 that the principle of thermal transpiration was applied to a device concept – the so-called Knudsen pump [4]. The promise of high structural efficiency because of no moving parts, high theoretical efficiency as compared to the conventional pumps, and favorable impact of high surface to volume ratio are some of the features of the Knudsen pump that are attractive for miniaturization.

The past two decades have seen the miniaturization of various devices like gas sampling and testing systems, vacuum cavity pressure control systems, etc. [5-9]. These devices utilize pumps that are often disproportionately large. Some efforts to miniaturize the pumps based on the conventional designs have been reported but most of them have reliability issues [10]. With the recent advances in micromachining technology, the field has seen new implementations of [11, 12] the Knudsen pump. One such effort is a fully micromachined

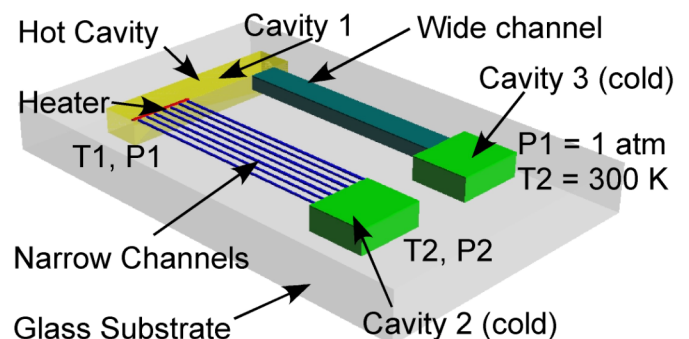


Fig. 1: 3D model for a single stage Knudsen pump.

Knudsen pump, which was reported by McNamara in 2005 [13]. This device (Fig. 1) achieves ≈ 0.46 atm. with 80 mW input power. While this effort demonstrated experimental feasibility, a predictive model was not reported.

This paper presents a modeling approach for a micromachined Knudsen pump. This involves numerical modeling of the thermal response, followed by an analytical estimate of the pumping using Kennard's model [14]. The results are subsequently validated against the previously reported experimental measurements of a single-stage Knudsen pump. The paper also extends the concept of single stage pumping to a multi-stage pump. While Kennard's model is used for modeling the first stage, the simulation for subsequent stages, which are characterized by a relatively high Knudsen number, uses an empirically corrected correlation by Knudsen [15]. For both single-stage and multi-stage pumps, the loss of performance resulting from gas diffusion through walls of the pump is specifically addressed [16].

The theory of operation of the Knudsen pump and the theoretical model for the phenomenon of thermal transpiration are discussed in section II, followed by a detailed description of the ANSYS thermal model in section III. Finally, section IV presents the simulation results, provides a comparative study with the experimental measurements and accounts for various non-idealities involved.

II. THEORY

Figure 2 illustrates the concept of thermal transpiration: a narrow channel, with hydraulic diameter less than the mean free path of the gas flowing through it, connects two chambers, one of which is maintained at higher temperature than the other. If both of these chambers have the same pressure initially, the equilibrium pressure in the cold chamber will be lower than that in the hot chamber. From the molecular dynamics point of view, it can be explained as an equilibrium state attained by two opposing flow fields, thermal creep flow and Poiseuille flow (Fig. 3). The former is the movement of the gas molecules near the wall as a consequence of the longitudinal temperature gradient in the channel. These molecules move from the cold end to the hot end, resulting in a pressure gradient along the channel, which causes a counter flow in the central part of the channel. This counter flow, known as Poiseuille flow, is induced by the pressure gradient generated by the thermal creep flow and it acts to nullify the same. At equilibrium, the two flows balance each other, resulting in a steady-state pressure gradient along the channel. This pressure gradient is not significant when the channel diameter is large compared to the molecular free path. However, an observable pressure gradient is generated if the hydraulic diameter of the channel is much smaller than the mean free path of the gas flowing through it, which permits a vanishingly small viscous domain for the Poiseuille flow.

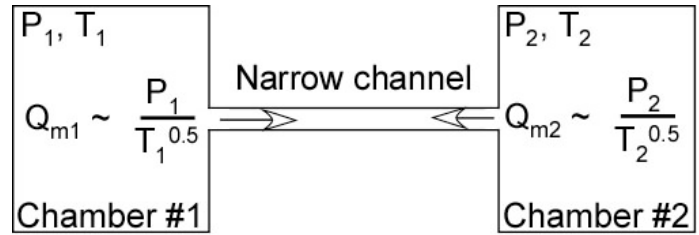


Fig. 2: Schematic demonstrating the thermal transpiration phenomenon.

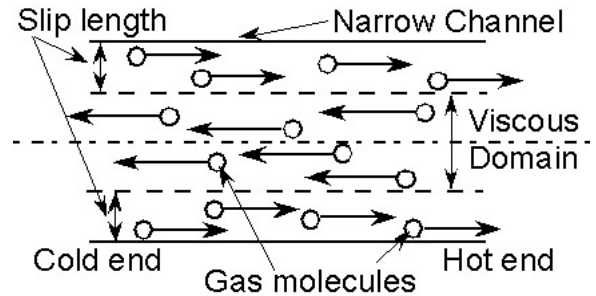


Fig. 3: Thermal transpiration at molecular level.

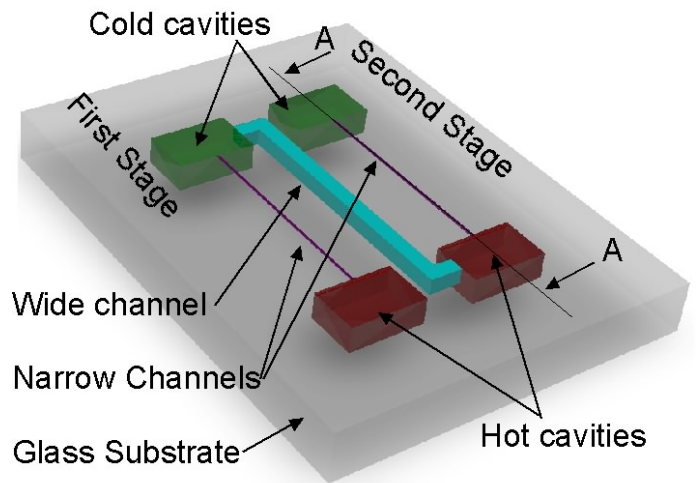


Fig. 4: 3D model for a two stage Knudsen pump.

This concept can further be extended to a multi-stage pump by cascading the hot and cold chambers in series, and connecting them by alternating narrow and wide channels. The cold cavity of a stage is connected to the hot cavity of the next stage through a wide channel, which allows gas flow in the viscous regime, thus enforcing the pressure in the two cavities to be the same (Fig. 4). The wide channel plays an important role in determining the lowest vacuum pressure that the device can attain. Once the mean free path of the gas at a particular stage exceeds the hydraulic diameter of the wide channel, the gas flow in the wide channel is no longer in viscous regime, thus rendering the successive stages ineffective. Under the

assumption that none of the wide channels experience rarefied gas flow, the minimum attainable pressure (P_{vac}) as a function of hot stage temperature (T_h), cold stage temperature (T_c), the outlet pressure (P_{outlet}), and the number of stages (s) is given by:

$$P_{vac} = P_{outlet} \left(\frac{T_c}{T_h} \right)^{\frac{s}{2}} \quad (1)$$

Since the gas flow in the narrow channels is in non-viscous flow regimes (i.e., the free molecular, transitional, or slip flow regimes) the modeling methodologies are based on the kinetic theory of gases. Most of the models used for the thermal transpiration are basically manifestations of by the Boltzmann equation:

$$\frac{\partial f}{\partial t} + \bar{v} \cdot \frac{\partial f}{\partial \bar{x}} + \bar{F} \cdot \frac{\partial f}{\partial \bar{v}} = Q(f, f_*) \quad (2)$$

where,

\bar{F} is the imposed body force,

\bar{v} is the velocity vector,

\bar{x} is the position vector,

f is the density function.

$\partial f / \partial t$ is the change in number of molecules in a region of space

$\bar{v} \cdot (\partial f / \partial \bar{x})$ represents molecules convected in or out of a region of space

$\bar{F} \cdot (\partial f / \partial \bar{v})$ convection of molecules due to body force

$Q(f, f_*)$ represents the effect of intermolecular collisions

The past century has seen various efforts [17-20] to theoretically model the principle of thermal transpiration and several attempts to validate these models based on the available experimental results [21-23]. Each of these models differs in the simplifying assumptions made for the term corresponding to intermolecular collision in Eq. 2, which is the primary constraint for a simple mathematical solution to the Boltzmann equation. The analysis presented in this paper uses the Kennard's model to estimate the pressure distribution across the narrow channel [14]:

$$U(y) = \frac{1}{4\mu} \frac{dP}{dx} [y^2 - a^2 - 2\xi a] + \frac{3}{4} \frac{\mu R}{P} \frac{\partial T}{\partial x} \quad (3)$$

where the terms on the left and right represent Poiseuille flow and thermal creep flow, respectively. Additionally,

$$\mu = \frac{1}{d^2} \sqrt{\frac{mk_B T}{\pi^3}} \quad (4)$$

$$a = \frac{wh}{w+h} \quad (5)$$

$$\lambda = \frac{1}{\sqrt{2\pi}Nd^2} \quad (6)$$

$$N = \frac{P}{k_B T} \quad (7)$$

$$\rho = mN \quad (8)$$

$$Kn = \frac{\lambda}{a} \quad (9)$$

In these equations, a is the hydraulic radius of the narrow channel, y is the distance from the wall of the channel where the flow velocity is being considered, P is the pressure of the gas, dP/dx is the corresponding pressure gradient, T is the temperature of the gas, dT/dx is the corresponding temperature gradient along the narrow channel, μ is the dynamic viscosity, R is the gas constant, d is the collision diameter of the molecule, m is the mass of the molecule, k_B is the Boltzmann constant, h is the height of the channel, w is the width of the channel, N is the number of molecules per unit volume, ρ is the density, Kn is Knudsen number, ξ is the slip length, which is equal to the mean free path λ for a purely diffusive reflection boundary condition. The fluid properties like viscosity, density depend on the local temperature and pressure of the gas but a simplified analysis may evaluate these for average values of temperature and pressure.

As background information, note that the free molecular, transitional, and slip flow regimes are represented by $Kn > 10$, $0.1 < Kn < 10$, and $0.01 < Kn < 0.1$, respectively [3]. Kennard's model assumes slip flow in channels of circular cross-section.

The velocity profile in Eq. 3 can be integrated to obtain the mass flow rate:

$$Q_m = -\frac{\pi}{8} \frac{a^4 P}{\mu R T} \frac{dP}{dx} \left[1 + 4 \frac{\xi}{a} \right] + \frac{3}{4} \frac{\mu a^2}{T} \frac{\partial T}{\partial x} \quad (10)$$

The negative term represents the counteracting natures of Poiseuille flow and thermal creep flow, which balance each other at equilibrium. Thus, at equilibrium, the pressure gradient across the two cavities can be represented by:

$$\frac{dP}{dx} = \frac{6R}{P} \frac{\mu^2}{a^2} \frac{\partial T}{\partial x} \left[1 + 4 \frac{\xi}{a} \right] \quad (11)$$

For the purposes of the numerical solution this can be discretized as:

$$\frac{P_{n+1} - P_n}{\Delta x} = \left[\frac{6R}{P} \frac{\mu^2}{a^2} \frac{\left(\frac{\partial T}{\partial x}\right)_n}{\left(1 + 4\frac{\xi}{a}\right)} \right]_{T_n, P_n} \quad (12)$$

where the subscript n signifies that the quantities are evaluated at the n^{th} node. The quantities on the right are evaluated for the temperature and pressure at n^{th} node, which is further used to solve for the pressure at the $(n+1)^{\text{th}}$ node. It can be seen from this representation that thermal creep effects can be significant in rarefied flows for which the pressure is low or in micro flows at the atmospheric pressures where the typical dimensions are of the order of mean free path of the gas.

While Kennard's model is potentially suitable for modeling the pressure distribution in a single stage pump, its validity for multi-stage pumps is questionable. This is because the pressure in the later stages is very low, resulting in transition or free molecular regime gas flow. Hence, an empirically corrected Knudsen's model is used to characterize the high Knudsen number flow in the subsequent stages of the multi-stage pump [15]:

$$\frac{dp}{dT} = \frac{1}{\frac{8}{3} \frac{1}{k_1} \frac{a}{\lambda} + \frac{\pi}{16} \left(\frac{0.81}{0.49}\right) \frac{a^2}{\lambda^2} \frac{1}{k_1}} \frac{p}{2T} \quad (13)$$

where k_1 is 1 for $Kn \gg 1$, else it converges to a value between 2 and 3. This model is appropriate for both free-molecular and transitional flow in narrow channels of circular cross-section.

In examining micromachined Knudsen pumps, one of the major concerns is the leakage of air through the walls of the channels or chambers. Egress or ingress of gas by this route can significantly affect performance because of the extraordinarily large ratio of surface area to volume. One mechanism of gas transport through the walls is simply diffusion. Diffusion can be important in chambers or channels that are heated and/or separated by a relatively thin wall from others at a significantly different pressure. The basic governing equation for diffusion of gas through a membrane is given by:

$$F = DS_m \frac{P_1^{0.5} - P_2^{0.5}}{l} \quad (14)$$

where F is the rate of diffusion per unit area of membrane, S_m is the solubility of gas ion the membrane, P_1 and P_2 are the pressures on the either side of the membrane, l is the thickness of the membrane, and D is the coefficient of diffusion through the membrane, which depends on the temperature of the membrane and is characteristic of the membrane material.

III. SIMULATION MODEL

Figure 5 shows the cross-sectional view of the Knudsen pump considered for the present analysis. The device has multiple narrow channels connecting two cavities (Fig. 1). The heated cavity is further connected through a wide channel to cavity 3, which remains at ambient. These large cavities ($160\mu\text{m} \times 50\mu\text{m} \times 10\mu\text{m}$) and the wide channel (cross-section: $30\mu\text{m} \times 10\mu\text{m}$), countersunk in a glass substrate, are capped by a $\text{SiO}_2/\text{Si}_3\text{N}_4/\text{SiO}_2$ stack (termed as dielectric stack), each layer being $0.3\mu\text{m}$ thick. The narrow channels (cross-section: $10\mu\text{m} \times 100\text{nm}$) have an additional micron-thick cap layer of polysilicon, which is also used for the hot cavity heater.

The thermal behavior of this device is modeled using ANSYS, which yields the results for the temperature distribution and corresponding gradient along the narrow channel. This model is also used to study the thermal losses from the model, which are indicative of power efficiency.

The temperature profile (Fig. 6) obtained from the ANSYS model serves as an input to the analytical model being used to estimate the pressure distribution along the channel. This step uses the analytical relations (Eq. 3-11) that characterize the effects of the thermal transpiration to estimate the pressure drop in the single stage Knudsen pump. The focus here is primarily on evaluating the relative location of various features like

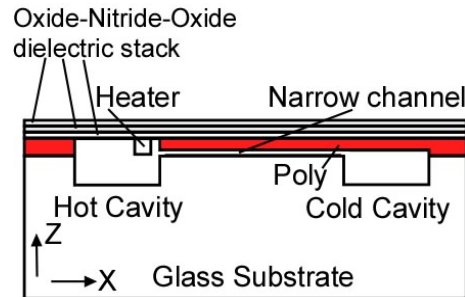


Fig. 5: Knudsen pump Section A-A of Fig. 4.

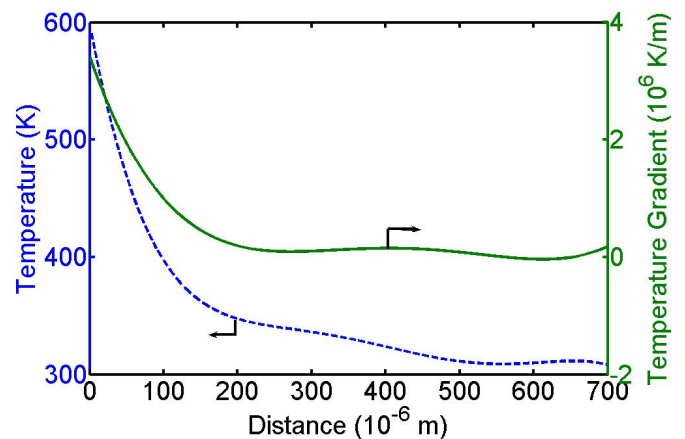


Fig. 6: Temperature and corresponding temperature gradient along the channel for a single stage pump.

cavities, flow channels and heaters on the device and their effect on the performance of the device. Later stages of the study address the impact of various non-idealities on the effectiveness of the Knudsen pump. This includes diffusion (Eq. 14) of gas through the structure, thermal contact resistance at the base of the device, etc. The analysis in this step highlights some of the sensitive design parameters for the Knudsen pump.

The model assumes a fixed temperature boundary condition at the base (i.e., the lower surface of the glass substrate), which is at thermal equilibrium with a heat sink at 300 K. The heater, located in the hot cavity, is maintained at 1373 K for simulation purposes. A convection boundary condition is imposed on the top and side faces of the device with ambient at 300 K. The air entrapped in the cavities and the narrow channel is modeled as a conducting solid (with thermal conductivity equal to that of air), which serves as a close approximation to the actual case because the most dominant mode of heat transfer is conduction through the substrate walls.

IV. RESULTS AND DISCUSSION

Single Stage Knudsen Pump – Temperature and Pressure

Figure 6 shows the temperature distribution along the narrow channel connecting the two cavities of the single stage Knudsen pump. A polynomial curve is fit through the nodal values of temperature from the ANSYS simulations. The polynomial expression used to fit the temperature is then differentiated to evaluate the temperature gradient along the channel. The interpolated data for the temperature distribution and corresponding gradient is further used to calculate the pressure gradient at various intermediate points in the channel. Figure 7 shows the pressure gradient and corresponding pressure distribution along the channel as predicted by the analytical model. The pressure in the hot cavity is assumed to be atmospheric because the cavity is vented to atmosphere through a second cold cavity (Fig. 1).

For the particular geometry evaluated, the modeling strategy described is successful in reproducing the experimental results with 80% accuracy. For the single stage Knudsen pump described above the analysis predicts a cold cavity pressure of 0.47 atm at input power of 97.6 mW, as compared to the experimental measurement of 80 mW for at a pressure of 0.46 atm. While there are many possible sources for the mismatch, one is related to the geometry of the narrow channels. As noted previously, Eqs. (11) and (13) are derived for channels of circular cross section. In the microfabricated device, however, the channels have a rectangular cross-section with an aspect ratio of 100:1. The calculations used an equivalent hydraulic diameter for these channels, which could lead to some error. While these initial results are encouraging, further validation will be sought in subsequent efforts.

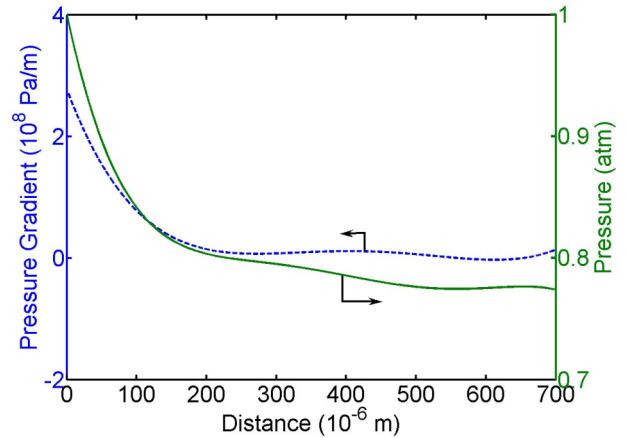


Fig. 7: Pressure gradient and corresponding pressure variation along the channel for the single stage Knudsen pump.

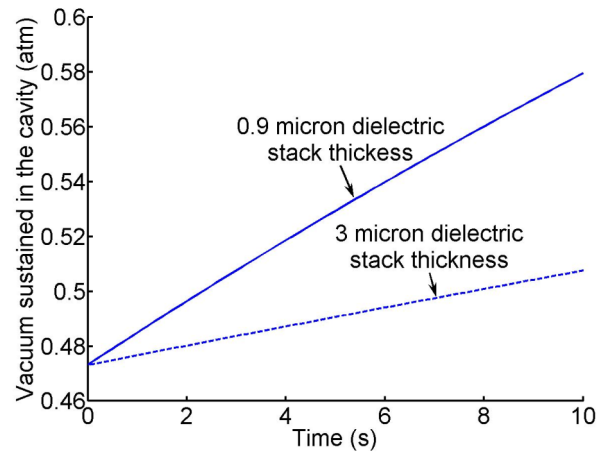


Fig. 8: Diffusion of air through dielectric stack of various thicknesses for the first stage of the multi-stage Knudsen pump.

A closer analysis of the temperature and pressure distribution suggests that the channel length of the Knudsen pump for these operating conditions can be reduced to about 200 μm without severely compromising the differential pressure achievable.

Diffusion

Figure 8 shows the progressive loss of the vacuum in the heated cavities (≈ 600 K) resulting due to the diffusion of gas through the walls. It suggests that if the dielectric stack thickness is tripled, the effects of diffusion can be diminished by 50%, which corresponds to an order of magnitude decrease in the leakage through the walls of hot cavities (Table I). For a multi-stage pump, beyond the first stage, the problem of leakage worsens because the heated cavities are substantially below atmospheric pressure, which increases the diffusion

through the dielectric stack. Table I enumerates the effect of diffusion of air into the unheated (≈ 300 K) and heated cavities. The gas diffusion rate into the former is three orders of magnitude lower than into the latter. This emphasizes the need to effectively insulate the heater from the dielectric stack; this has the potential to improve the performance by at least two orders of magnitude.

Thermal Contact Resistance

In order to assess the impact of poor thermal contact between the lower surface of the glass substrate and the heat sink or chuck upon which it is located, a separate analysis was performed. A thin film of air with thickness of the order of surface asperities ($0.1-0.5 \mu\text{m}$) was assumed to exist between the glass substrate and the (fixed temperature) heat sink. Examining heat loss due to conduction alone, it was found that this did not have significant impact upon the performance of the pump. The thermal resistance added by this layer of air is relatively small because it has a short length and a large cross-sectional area ($1500 \times 2000 \mu\text{m}^2$).

Table I: Leakage rates corresponding to the various dielectric thicknesses and temperatures at a cavity pressure of 0.47 atm.

Temperature (K)	Dielectric Thickness (μm)	Leakage Rate (cc/sec)
310	0.9	7.1×10^{-12}
650	0.9	2.2×10^{-9}
650	3	6.7×10^{-10}

Multi-Stage Pumps

Table II presents an analysis of a three stage Knudsen pump. It lists the pressure in the heated cavities (P_h), pressure in the unheated cavities for the case that no leakage occurs ($P_{c-no\ leak}$), and pressure in the unheated cavities after having accounted for the air leakage ($P_{c-actual}$). The loss in vacuum in the unheated cavities is primarily due to the inflow of gas into them from the heated cavity of the next stage through the wide channel connecting them. For this reason, the unheated cavity of the final stage, which is not connected to a heated cavity in a succeeding stage, does not change in pressure significantly when diffusion is taken into account. The three-stage pump studied here is expected to attain a vacuum pressure of 0.28 atm. for an input power of 290 mW.

Table II: Analysis for a three-stage Knudsen pump, comparing the pressure in the heated cavities (P_h) to that in unheated ones in the absence of leakage ($P_{c-no\ leak}$), and to the actual one ($P_{c-actual}$) which accounts for gas diffusion.

Stage	P_h (atm)	$P_{c-no\ leak}$ (atm)	$P_{c-actual}$ (atm)
1 st	1	0.47	0.50
2 nd	0.50	0.39	0.40
3 rd	0.40	0.28	0.28

V. CONCLUSION

The study shows that the Kennard's model can a suitable tool for modeling the thermal transpiration phenomenon in single stage planar Si-micromachined Knudsen pumps and in the first stage of multi-stage pumps, for which the gas flow is in the slip flow regime. Knudsen's model is more appropriate for subsequent stages in multi-stage pumps, for which flow is not in the slip domain; in these cases Kennard's model yields unrealistic pressures. The analysis highlights some important design strategies that can provide more effective pumping. These include, for example, reducing the length of narrow channels to $200 \mu\text{m}$ in the fabrication process described here, improving isolation of the heater from the dielectric stack, managing leakage in multi-stage pumping.

Moving forward, the models presented here will be benchmarked against others that can evaluate thermal transpiration at all values of Kn . Both analytical and numerical models [24-27] will be explored. Some, like Sharipov's model, use numerically determined flow coefficients to model the flow through the narrow channel. A Monte Carlo technique based on the simulation of the molecular dynamics in the narrow channel is also promising.

ACKNOWLEDGMENT

The authors would like to thank Prof. Wenjing Ye of Georgia Institute of Technology, Atlanta, GA for valuable discussions. NG acknowledges the graduate student fellowship awarded by the Department of Mechanical Engineering, University of Michigan, Ann Arbor, which was the primary source of support for this work.

REFERENCES

- [1] Reynolds, O., 1878, "On Certain Dimensional Properties of Matter in the Gaseous State," *Philos. Tran. Royal Society London*, **170**, pp. 727-845.
- [2] Maxwell, J. C., 1879, "On Stresses in Rarefied Gases Arising from Inequalities of Temperature," *Philos. Tran. Royal Society London*, **170**, pp. 231-256.
- [3] Karniadakis, G. E., Beskok, A., and Aluru, N., 2005, *Microflows and Nanoflows: Fundamentals and Simulation*, Springer, New York, Chap. 1.
- [4] Knudsen, M., 1910, "Eine Revision der Gleichgewichtsbedingung der Gase. Thermische Molecularströmung," *Ann. Phys., Leipzig*, **31**, pp. 205-229.
- [5] Kolesar, E. S., Jr., Spangler, G. E., 1998, "Review and Summary of a Silicon Micromachined Gas Chromatography System," *IEEE Transactions on Components Packaging and Manufacturing Technology, Part B: Advanced Packaging*, **21**(4), pp. 324-328.
- [6] Lu, C. J., Tian, W. C., Steinecker, W. H., Guyon, A., Agah, M., Oborny, M. C., Wise, K. D., Pang, S. W., and Zellers, E. T., 2003, "Functionally Integrated MEMS Micro Gas Chromatograph Subsystem," *7th Intl. Conference of Miniaturized Chemical and Biochemical Analysis Systems*, pp. 411-415.

- [7] Agah, M., Potkay, J. A., Lambertus, G., Sacks, R., and Wise, K. D., 2005, "High-Performance Temperature Programmed Microfabricated Gas Chromatography Columns," *Journal of Microelectromechanical Systems*, **14**(5), pp. 1039-1050.
- [8] Kolesar, E. S., Jr., and Spangler, G. E., 2001, "Advances in Fabricating Silicon Micromachined Gas Chromatographic Columns," *Twenty-Fourth International Symposium of the American Chemical Society (ACS) on Capillary Chromatography and Electrophoresis*, Las Vegas, NV.
- [9] Tian, W. C., Pang, S. W., Lu, C.-J., and Zellers, E. T., 2003, "Microfabricated Preconcentrator-Focuser for a Microscale Gas Chromatograph," *Journal of Microelectromechanical Systems*, **12**(3), pp. 264-272.
- [10] Nguyen, N. T., Huang, X., Chuan, T. K., 2002, "MEMS-Micropumps: A Review," *ASME J. Fluid Eng.* **124**(22), pp. 384-392.
- [11] Vargo, S. E., Muntz, E. P., Shifflett, G. R., 1999, "Knudsen Compressor as a micro- and macroscale vacuum pump without moving parts or fluids," *J. Vac. Sci. Technol.*, **A17**(4), pp. 2308-2313.
- [12] Vargo, S. E., Muntz, E. P., 2001, "Initial results from the first MEMS fabricated thermal transpiration-driven vacuum pump," *Rarefied Gas Dynamics, AIP Conference Proceedings*, **585**, pp. 502-509.
- [13] McNamara, S., and Gianchandani, Y. B., 2005, "On-Chip Vacuum Generated by a Micromachined Knudsen Pump," *J. Microelectromechanical Systems*, **14**(4), pp. 741-746.
- [14] Kennard, E. H., 1938, *Kinetic Theory of Gases*, McGraw Hill, pp. 327-332.
- [15] Loeb, L. B., 1934, *The Kinetic Theory of Gases*, McGraw Hill, pp. 355-359.
- [16] Hwang, S.-T., Kammermeyer, K., 1974, "Membranes in Separation," *Techniques of Chemistry*, Vol. VII, John Wiley Sons, Chap. VI.
- [17] Williams III, J. C., 1970, "Thermal Transpiration – A Continuum Gasdynamics View," *J. Vac. Sci. Technol.*, **8**, pp. 446-450.
- [18] Ebert, W. A., and Sparrow, E. M., 1965, "Slip flow in rectangular and annular ducts," *J. Basic Eng.*, **87**, p. 1018-1024.
- [19] Morini, G. L., and Spiga, M., 1998, "Slip flow in rectangular microtubes," *Microscale Therm. Eng.*, **2**(4), pp. 273-282.
- [20] Aubert, C., and Colin, S., 2001, "Higher order boundary conditions for gaseous flows in rectangular microchannels," *Microscale Therm. Eng.*, **5**(1), pp. 41-54.
- [21] Colin, S., Lalonde, P., and Caen, R., 2004, "Validation of a second order slip flow model in rectangular microchannels," *Heat Transfer Eng.* **25**(3), pp. 23-30.
- [22] Maurer, J., Tabling, P., Joseph, P., and Willaime, H., 2003, "Second order slip laws in microchannels for helium and nitrogen," *Phys. Fluids*, **15**(9), pp. 2613-2621.
- [23] Arkilic, E. B., Breuer, K. S., and Schmidt, M. A., 2001, "Mass flow and tangential momentum accommodation in silicon micromachined channels," *J. Fluid Mech.*, **437**, pp. 29-43.
- [24] Bhatnagar, P., Gross, E., and Krook, K., 1954, "A model for collision processes in gases," *Phys. Review*, **94**, pp. 511-524.
- [25] Sharipov, F., 1999, "Non-isothermal gas flow through rectangular microchannels," *J. Micromechanics and Microengineering*, **9**, pp. 394-401.
- [26] Bird, G. A., 1994, *Molecular Gas Dynamics and the Direct Simulation of Gas Flows*. Oxford, UK.
- [27] Oran, E. S., Oh, C. K., Cybyk, B. Z., 1998, "Direct Simulation Monte Carlo: Recent Advances and Applications," *Annu. Rev. Fluid Mech.*, **30**, pp. 403-441.0